Broad-Band Fragmented Aperture Phased Array Element Design Using Genetic Algorithms

Björn Thors, Hans Steyskal, *Fellow, IEEE*, and Henrik Holter

***Abstract*—In this paper, a synthesis procedure to design thin broad-band fragmented aperture array elements is described. The arrays are assumed to be infinite periodic and the elements consist of a conducting pattern etched on a dielectric backed by a groundplane. A genetic algorithm (GA) is used to design the conducting pattern, relative permittivity, and thickness of the dielectric substrate with respect to array scan and bandwidth performance. The fitness function in the GA is evaluated using a finite-difference time-domain code with periodic boundary conditions. For a substrate thicker than about 0.1 λ_L (λ_L = wavelength at the lowest frequency in the frequency band investigated), it was found that a bandwidth of at least one octave can be obtained for arrays scanned within 45° from broadside.**

***Index Terms*—Broad-band antennas, finite-difference time-domain (FDTD), genetic algorithm (GA), phased arrays.**

I. Introduction

BROAD-BAND array antennas are becoming increasingly important for military as well as commercial applications. Sometimes it is claimed that a truly broad-band array can only be obtained if all the array dimensions are fully exploited. The interelement spacing is determined by the condition that no grating lobes appear over the frequency and scan range, while the size of the total aperture is determined by the desired directivity. The extension in depth, however, is different for different types of elements, and presently there is no known relationship between bandwidth and the minimum depth of the antenna.

The best known wide-band array elements, the tapered slot [1], the TEM-horn [2], the bunny-ear antenna [3], and the body-of-revolution (BOR) element [4], are three-dimensional elements that use the dimension normal to the aperture plane. These elements usually have a depth of 0.1–0.25 λ_L, where λ_L is the wavelength at the low end of the frequency band.

Planar, two-dimensional elements offer a simplified geometry and potentially simplified manufacturing and flush, conformal mounting. Due to mutual coupling, dipole arrays can be designed to operate over much larger bandwidths than an individual element. Dense arrays of wire dipoles have been analyzed [5], [6], similar arrays where the dipole arms consist of circular patches [7], [8] and wide crosses [9] have been proposed, and recently a wide-band dipole array was presented [10]. In most cases, however, design guide lines and results are scant or nonexistent. Therefore, this paper explores a design approach for a planar patch phased array element with octave bandwidth.

Genetic algorithms (GAs) have been used to optimize the shape of patch elements, both as single elements [11] and as phased array elements [12]. In [12], the optimization was based on a GA in combination with a stochastic hill climbing technique and led to a fragmented aperture design. However, most of the numerical examples given in [12] are for arrays without a groundplane, which means that the resulting arrays radiate in two directions. No results are given for groundplane backed arrays scanned off broadside. In this paper, a similar genetic algorithm is used to synthesize a broad-band groundplane backed fragmented aperture array scanned within 45° from broadside.

This paper focuses on the broad-band properties of the arrays investigated and not on the optimization method. A detailed description of the GA can be found in [13].

II. GA Synthesis Procedure

A key step in the GA lies in the evaluation of the fitness function. Since we are interested in designing a broad-band array, it seems reasonable to define a fitness function that minimizes the standing wave ratio (SWR) over a large frequency range. This implies that the SWR must be calculated for many frequencies. Furthermore, many geometries will have to be analyzed during the design procedure which necessitates a fast electromagnetic solver. The problem is simplified by approximating the large array antenna with an infinite periodic array for which a unit cell analysis suffices. For the analysis, a finite-difference time-domain (FDTD) program with periodic boundary conditions is used [14]. The geometry of the unit cell is shown in Fig. 1.

The design goal is to find a distribution of conducting regions on the aperture surface, which together with a suitably chosen permittivity and thickness of the dielectric substrate will produce a well-matched antenna over a large frequency range for all scan directions. In order to search for the optimum distribution of conducting regions, the unit cell aperture is gridded into 20×20 pixels where each pixel can be assigned either conducting or nonconducting properties. The element is fed by a voltage source in the center of the unit cell and the conducting regions are constrained to be symmetric around the feed point.

Manuscript received September 22, 2004; revised April 14, 2005.

B. Thors was with the Division of Electromagnetic Theory, Royal Institute of Technology, SE-100 44 Stockholm, Sweden. He is now with Ericsson Research, KI/EAB/TFF, SE 164 80 Stockholm, Sweden (e-mail: bjorn.thors@ericsson.com).

H. Steyskal was with the Division of Electromagnetic Theory, Royal Institute of Technology, SE-100 44 Stockholm, Sweden. He is now with the Air Force Research Laboratory, Hanscom AFB, MA 01730 USA (e-mail: hans.steyskal@hanscom.af.mil).

H. Holter is with Saab Bofors Dynamics AB, SE-175 88 Stockholm, Sweden (e-mail: henrik.holter@dynamics.saab.se).

Digital Object Identifier 10.1109/TAP.2005.856340

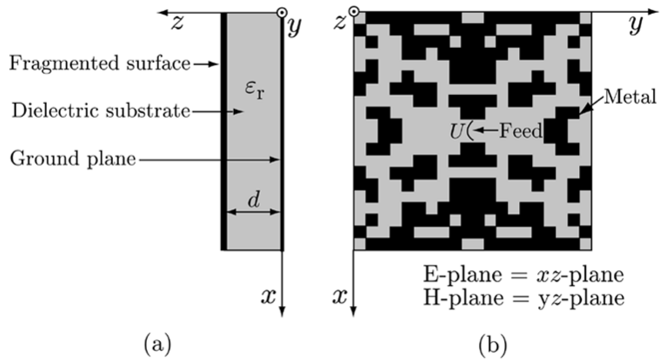

Fig. 1. Unit cell geometry for a random fragmented aperture array. (a) Side view and (b) top view.

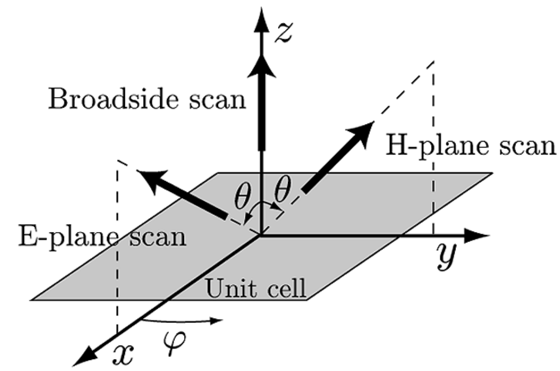

Fig. 2. Scan directions used to evaluate the antenna elements.

Thus, only a quadrant of the unit cell will be coded as genes in the GA.

The quadratic pixels in the 10×10 quadrant are numbered from 1 to 100. Since only two values are possible for each region (conducting or nonconducting), a binary coding is practical and the entire fragmented aperture is described by the first 100 bits in the chromosomes. If more parameters are included in the design, such as the relative permittivity and/or the substrate thickness, the corresponding genes are just added after the first 100 bits in the chromosomes.

Since the antenna impedance varies with scan direction, the performance of the antenna elements will be evaluated for three different scan directions according to Fig. 2.

In this paper, an SWR≤ 2 (reflection coefficient $\lessapprox -9.5$ dB) is used as the criterion for a well-matched antenna. Thus, the bandwidth BW is defined as the ratio of the frequencies f_H and f_L $(f_H > f_L)$ between which SWR≤ 2 for all scan directions.

As mentioned before, the definition of the fitness function has to reflect the desired properties of the design. In the numerical simulations in Section III, the sum of the reflected energy for the three scan directions is minimized over a certain frequency band (design band) B_d. Thus, a suitable choice for the fitness function, which is to be maximized, is

$$F = -\sum_i \sum_j w_{ij} \left|\Gamma(\Omega_i, f_j)\right|^2 \tag{1}$$

where f_j denotes the discrete sample frequencies over the design band and Ω_i denotes the different sample scan directions. Different types of weighting functions have been used in the simulations, which are represented by the coefficients w_{ij}. The design band B_d must not be made too large since the fitness function should correspond to a realistic design objective.

III. Numerical Results

The elements are placed in a square grid with an element spacing $\Delta L = 3$ cm in the two principal directions. For the numerical results in Section III-A and B, the arrays are scanned to broadside $(\theta = 0^\circ)$ and to $\theta = 45^\circ$ in the cardinal planes. The corresponding frequencies where grating lobes will start to propagate are $f = 10.0$ and 5.86 GHz, respectively.

A. Arrays Without Groundplane

In 1948, Mushiake observed that antennas with a self-complementary structure[1] have an input impedance equal to half the intrinsic impedance of space, independent of the frequency and the shape of the structure [15], [16]. For array antennas, grating lobes will eventually appear when the frequency is increased, which will modify the input impedance and limit the bandwidth. Moreover, the input impedance will also depend on the scan angle, which might further reduce the performance of the array. An example of an approximately self-complementary array of square patches is shown in Fig. 3(a) [2]. Due to the staircase approximation in standard FDTD, the element is not strictly self-complementary—only 184 of the 400 pixels are conducting. Array feeding is across the corners of adjacent patches. The active reflection coefficient for this self-complementary array as computed by our periodic boundary (PB)-FDTD code [14] is given in Fig. 3(b).

The PB-FDTD code used for the analysis calculates the antenna impedance as a function of frequency. The reflection coefficients shown in Fig. 3(b) were then obtained by relating this impedance to the characteristic impedance of an imagined transmission line feeding the antenna. The characteristic impedance Z_c used to produce the results in Fig. 3(b) was set to $Z_c = Z_0/2$, where Z_0 denotes the intrinsic impedance of free space. As expected, for broadside scan, the array is very well matched for this value of Z_c. When the array is scanned in the E- and H-plane, the antenna impedance is changed (see, e.g., [17]) but the array is still well matched up to frequencies where grating lobe effects appear.

This self-complementary element, which has optimal frequency performance at broadside, was based on physical insight. Therefore, an interesting question is: How does this design compare with a GA design? Fig. 4 shows results for an array where the metal distribution was designed to produce a low reflection coefficient within the design band $B_d = 0.5$–5.0 GHz.

Apparently the metal distribution obtained is quite different from the self-complementary geometry in Fig. 3(a). The results for the reflection coefficients, however, are rather similar compared to the corresponding results for the self-complementary array. We have been found that different simulations in the end

[1]The shape of a self-complementary planar antenna is identical to that of its complementary antenna.

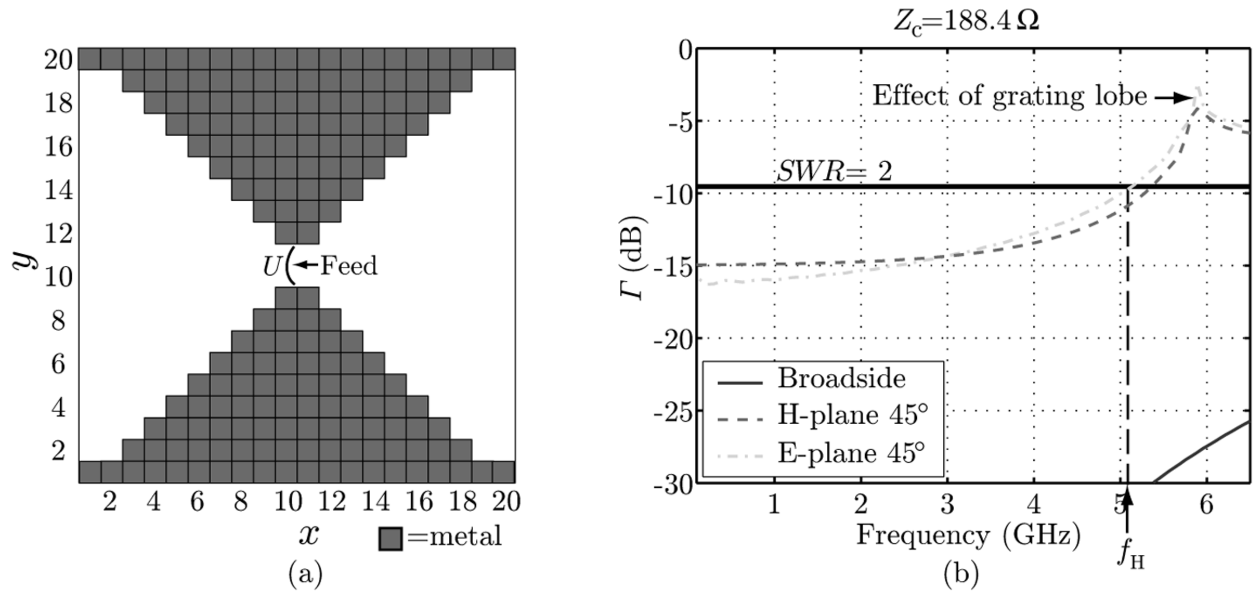

Fig. 3. Self-complementary array. (a) Unit cell geometry and (b) reflection coefficients.

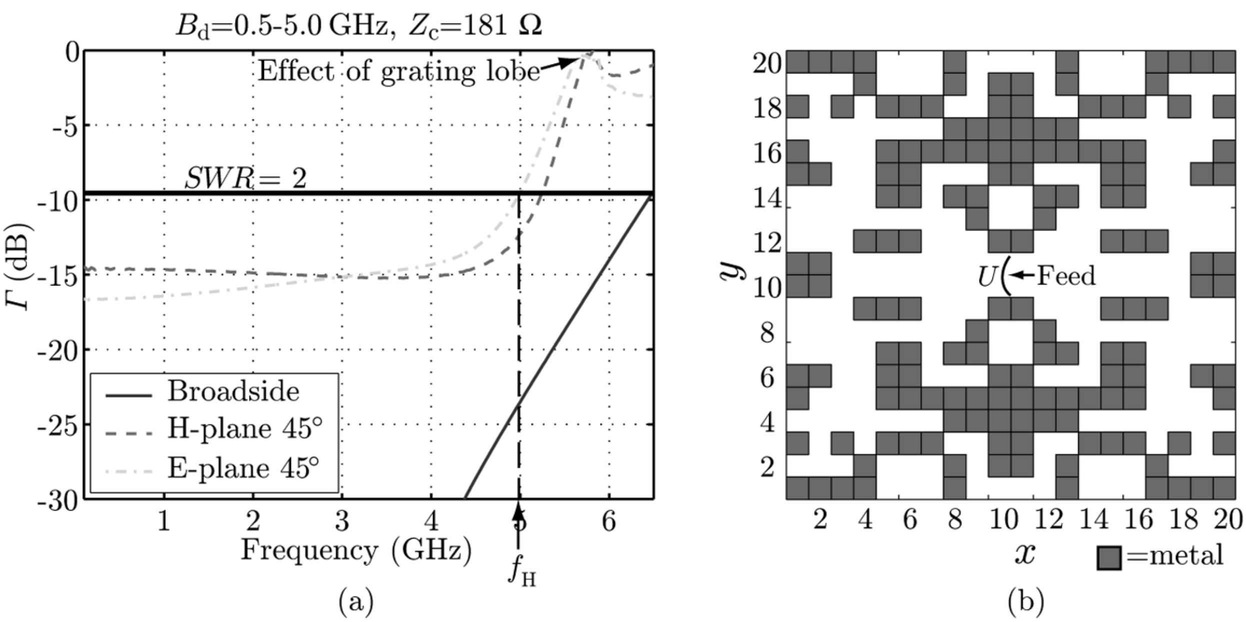

Fig. 4. Design results for an array antenna without a groundplane. (a) Reflection coefficients and (b) unit cell geometry.

usually lead to different geometries but with similar impedance characteristics. These were all "fragmented" patches, and in no case was a single solid patch like in Fig. 3(a) found. In other words, the search space seems to consist of several local maxima of similar fitness. (There are 2^{100} possible aperture configurations in total.)

B. Arrays With Groundplane

As shown in the previous section, extremely broad-band array antennas can easily be designed for the case of no supporting groundplane. This is, however, mostly of academic interest since their bidirectional radiation characteristics limit their range of applications. For groundplane backed arrays, no simple broad-band designs are available and more effort (analytical and/or computational) must be invested in the design.

1) Design of Element Configuration and Substrate Permittivity: In this section, a GA is used to design the patch shape and the dielectric substrate of a groundplane backed fragmented aperture array. The relative permittivity of the substrate ε_r was allowed to take 16 discrete values in the range 1.1–4.0, while the corresponding conductivity σ always was set equal to zero. From a broad-band perspective, the largest difference between groundplane backed arrays and arrays without groundplane is that the groundplane constitute a bandwidth limiting factor at low frequencies. At high frequencies the bandwidth is limited, for both array types, by grating lobe effects. Thus, in an attempt to favor antennas well matched in the center of the design band, the reflection coefficients were weighted with a half-period of a sine function. The sine function was designed to go to zero 0.5 GHz outside the bounds of the design band. It was felt

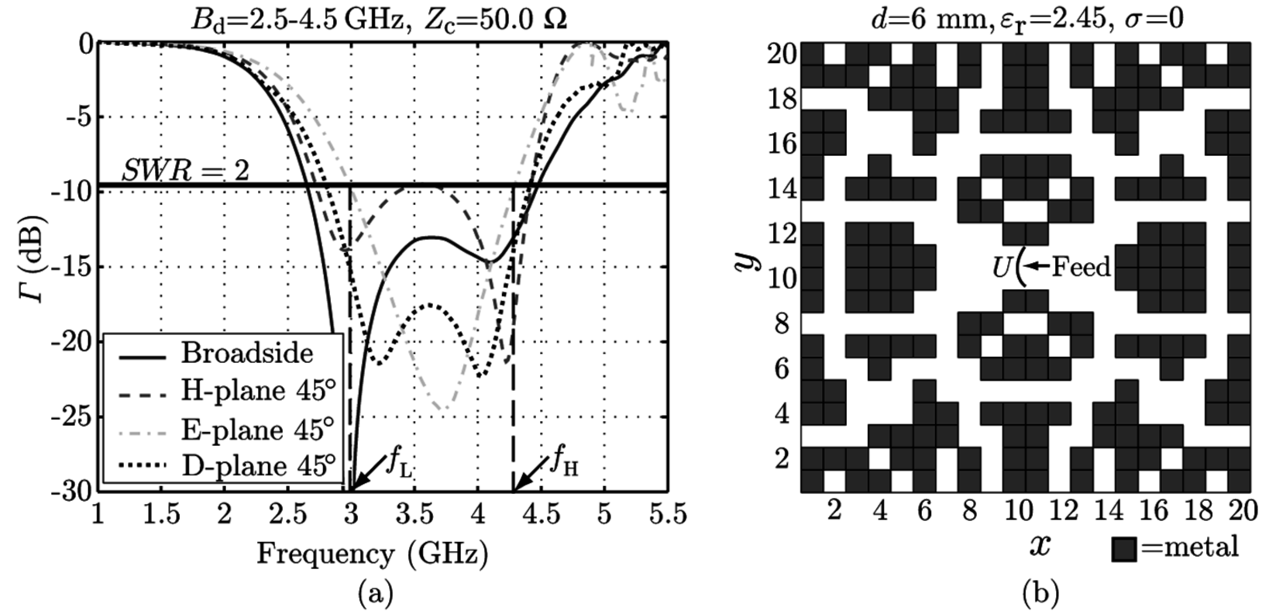

Fig. 5. Design results for a thin array antenna ($d = 6$ mm, design $B_d = 2.5$–4.5 GHz, obtained BW= $1.43 : 1$). (a) Reflection coefficients and (b) unit cell geometry.

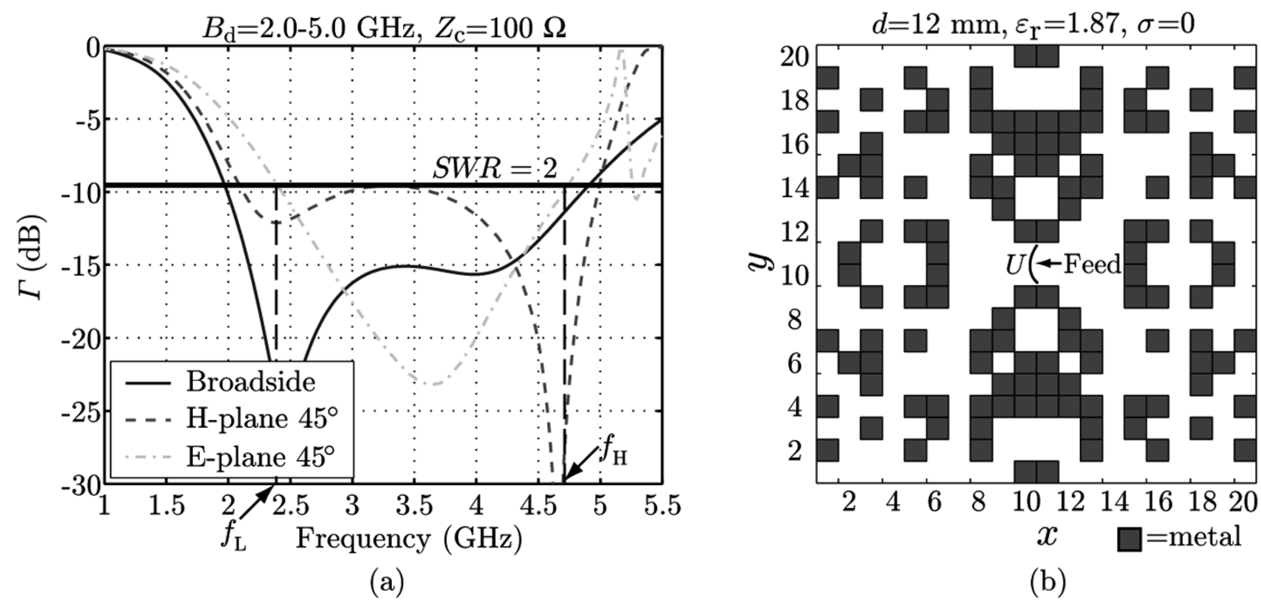

Fig. 6. Design results for an array antenna with $d = 12$ mm (design $B_d = 2.0$–5.0 GHz, obtained BW= $1.98 : 1$). (a) Reflection coefficients and (b) unit cell geometry.

that this approach would provide a better indication of achievable bandwidth than trying to force a uniform but, perhaps, poor match over the entire band. In the previous section, where the bandwidth was limited only for high frequencies, a uniform weighting function was used.

Fig. 5 shows results when the metal distribution and the relative permittivity of the substrate were designed for a thin element (substrate thickness $d = 6$ mm $= 0.07\,\lambda$ at center frequency) within the frequency band $B_d = 2.5$–4.5 GHz.

As expected, the groundplane constitutes a bandwidth limiting factor at low frequencies, and, with the thin substrate considered above, a bandwidth of about 1.43:1 was obtained. As mentioned before, the performance of the arrays is evaluated for three different scan directions according to Fig. 2 ($[\theta = 0°]$, $[\theta = 45°, \varphi = 0°]$, $[\theta = 45°, \varphi = 90°]$). In practice, however, it is often required that the arrays perform well also for intercardinal plane scanning. In Fig. 5(a), numerical results are also given with the array scanned to $\theta = 45°$ in the diagonal plane ($\varphi = 45°$). The diagonal plane is located between the cardinal planes, and it is therefore not surprising that the dotted curve in Fig. 5(a) is located " between" the cardinal plane curves. It should be emphasized that diagonal plane scanning cannot be considered as a linear combination of scanning in the cardinal planes. Nevertheless, based on experience from numerous simulations, arrays that perform well for cardinal plane scanning are likely to perform well also for diagonal plane scanning for fre-

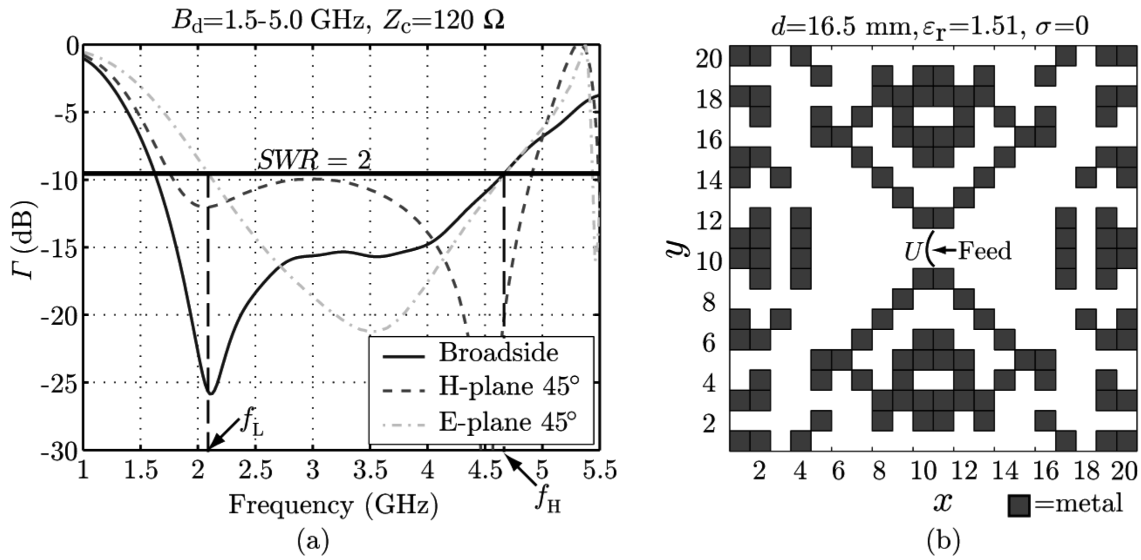

Fig. 7. Design results for an array antenna when the substrate thickness was allowed to take values between 6.0–28.5 mm. (Design $B_d = 1.5$–5.0 GHz, obtained BW= $2.23:1$.) (a) Reflection coefficients and (b) unit cell geometry.

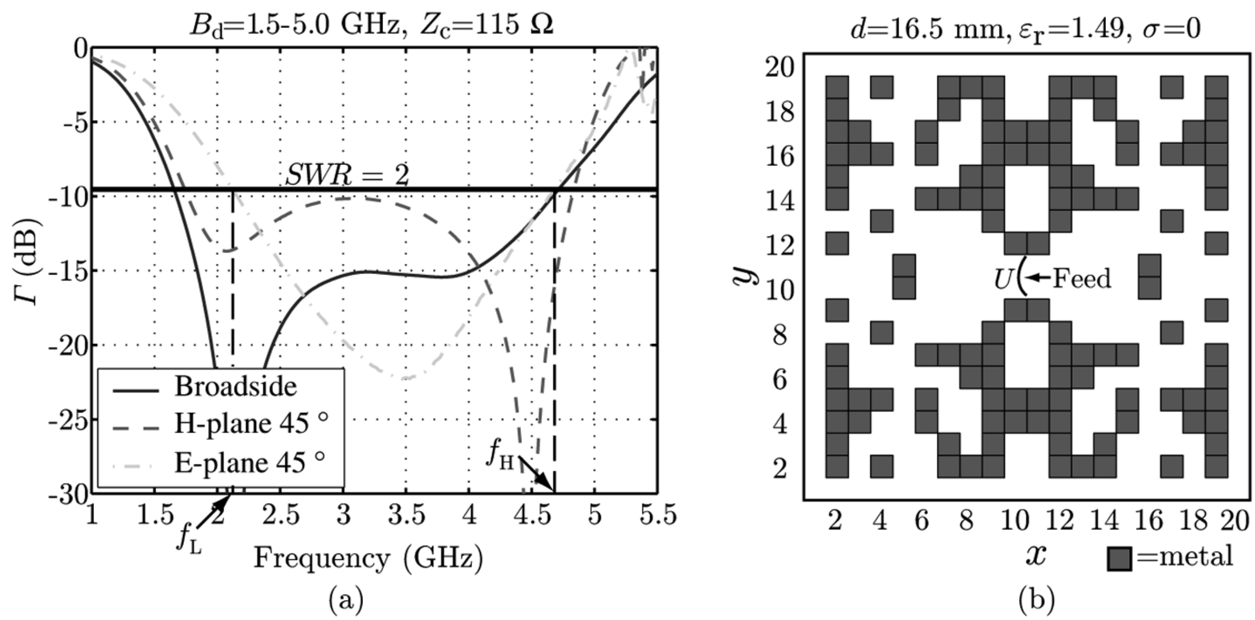

Fig. 8. Design results for an array antenna with element contact restricted. ($B_d = 1.5$–5.0 GHz, $d = 16.5$ mm, BW= $2.21:1$). (a) Reflection coefficients and (b) unit cell geometry.

quencies where no grating lobes can propagate. Thus, the simplification of omitting diagonal plane scanning when evaluating the array fitness may be justified.

The reflection coefficients presented in this section were obtained by relating the antenna impedance to a characteristic impedance of 50 Ω. From a broad-band perspective, however, this value of Z_c might not be the optimal choice. From now onwards, the characteristic impedance is allowed to take values between 20–300 Ω. This is accomplished by assuming a set of 281 evenly spaced, fixed values for Z_c and computing the corresponding fitness according to (1) for each of these fixed values. For each element configuration, this leads to a set of fitness values with corresponding Z_c values, from which the best Z_c value is chosen. Thus, the characteristic impedance is not encoded and included in the GA chromosomes. In Fig. 6, results are given for an array with $d = 12$ mm ($\approx 0.14\ \lambda$ at center frequency).

By increasing the substrate thickness, the impedance match is improved within the design band, which results in a bandwidth of practically one octave.

2) Design of Element Configuration, Substrate Permittivity, and Thickness: All results presented so far in this section have been obtained for a fixed value of the substrate thickness. One natural extension is to include this thickness in the fitness function. In Fig. 7, some design results are presented when the substrate thickness was allowed to take 16 discrete values between 6.0–28.5 mm, 0.065–0.31 λ at center frequency. As expected, by including the substrate thickness in the GA, a better impedance

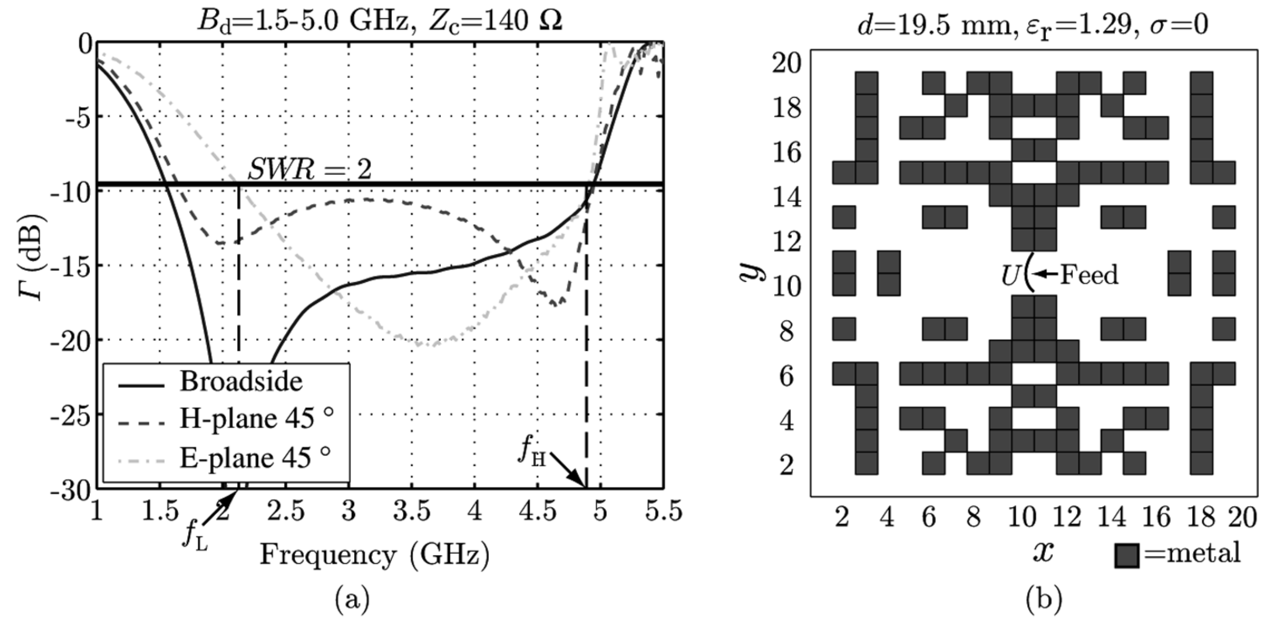

Fig. 9. Design results for an array antenna with element contact restricted when the substrate thickness was allowed to take values between 6.0–28.5 mm. ($B_d = 1.5$–5.0 GHz, BW= $2.32:1$). (a) Reflection coefficients and (b) unit cell geometry.

match was obtained compared to the results obtained previously for fixed values of d and the obtained bandwidth BW= $2.23:1$.

IV. Effects of Interelement Contact

In the literature [12], it has been suggested that electrical contact between adjacent elements sometimes can be advantageous for the matching properties at low frequencies. This is explained by noting that the elements are then not electrically confined within the unit cell. For the designs above, no restrictions regarding electrical contact were placed on the elements and the GA was left to find the best way to connect the elements and account for the interelement coupling. By restricting the elements from contacting each other, the possible advantage with a connected array can be studied. In Fig. 8, results are given for an array antenna when the outermost part of each unit cell was forced to be nonconducting. The parameter settings used for the design were identical to the settings used in Fig. 7, except that the substrate thickness was fixed to 16.5 mm.

By comparing Fig. 8(a) with Fig. 7(a), it is evident that the matching properties changed very little by preventing element contact. Thus, it seems that element contact is not so important for this type of antenna.

In Fig. 8, the design was made with d fixed to 16.5 mm corresponding to the substrate thickness obtained in Fig. 7. Another interesting question is how an unconnected design will perform if the substrate thickness is included in the design. This is illustrated in Fig. 9, where it is shown that the substrate thickness increased to 19.5 mm by allowing the GA to search between 6.0–28.5 mm. A bandwidth of 2.32:1 was obtained for the new design as a result of shifting f_H to higher frequencies.

It is also interesting to note that the bandwidth obtained in Fig. 9 actually is larger than the bandwidth obtained in Fig. 7. Since arrays with restricted element contact constitute a subset of all possible arrays, the GA should in theory be able to find such a design if it has a higher fitness value, as well as when element contact is allowed. However, by forcing the outermost pixels of the unit cell to be nonconducting, the number of possible aperture configurations is reduced by a factor of 2^{19}. Thus, it seems reasonable that the convergence properties are better for the unconnected case. All simulations in this paper were run until no significant improvement in convergence was observed for a very long time. However, since the GA to a large extent is based on randomness, there is no guarantee that the obtained solution is the most optimum solution. This is especially true for the current problem, where several local maxima of almost the same fitness exist within the search space. The results in Fig. 9 confirm the conclusion that electrical contact between neighboring elements not necessarily will improve the performance of the array.

V. Computational Comments

In contrast to [11], which used a cluster supercomputing platform for designing a single patch element, we designed our phased array element on a standard 2.26 GHz PC. A typical run took about 25 h until convergence.

To validate the results obtained by our code PB-FDTD, we analyzed the broadside scan array in Fig. 6(b) also with the commercial code CST MICROWAVE STUDIO (CST-MS). A comparison between the two codes is given in Fig. 10. The PB-FDTD results were obtained for two different meshes: a relatively coarse mesh (36 cells/wavelength at 5.5 GHz) corresponding to the mesh used in the GA (where computational speed is important) and a significantly finer mesh (436 cells/wavelength at 5.5 GHz) used to obtain convergence. As shown in Fig. 10, by using a finer mesh, the curve for the reflection coefficient is shifted upwards in frequency. The general shape of the curve, however, has not changed much, and we conclude that the mesh density used for the GA will produce reasonable results, which can be used to roughly predict the performance

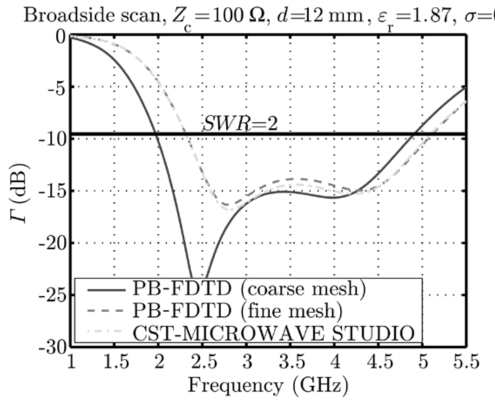

Fig. 10. Comparison between PB-FDTD and CST-MS for the array in Fig. 6(b) scanned to broadside. The coarse mesh corresponds to 36 cells/wavelength at 5.5 GHz while the fine mesh corresponds to 436 cells/wavelength at 5.5 GHz.

of the array. When a GA design has been obtained, a detailed analysis can easily be made by increasing the number of cells.

As shown in Fig. 10, the agreement between the PB-FDTD results (fine mesh) and the CST-MS results is quite good. It is interesting to note that the computational domain had to be discretized into a huge number of cells, both for PB-FDTD and CST-MS, in order to obtain convergence. This can perhaps be explained by the rectangular shapes in the fragmented aperture, where neighboring conducting regions sometimes only are connected at the corners of two pixels. For the lossless case analyzed in this paper, this could result in large current densities and high reactive power that need to be accurately modeled in order to obtain convergence.

The possibly large current densities at the corners of two pixels could perhaps in some cases also give rise to ohmic losses, which will degrade the performance of the array. In [18], a detailed sensitivity analysis was presented in which one pixel was added or removed in various locations within each quadrant of the unit cell. This analysis indicates that a slightly changed electric contact between different regions of the unit cell only will have a minor effect on the matching properties. Thus, it seems reasonable to expect that the connections at the corners between different pixels can be given a finite width if a prototype array is manufactured in the future.

VI. Conclusion

In this paper, a genetic algorithm has been used to synthesize broad-band fragmented aperture array elements for scan angles within 45° from broadside. Numerical simulations show that different designs in the end often lead to different element configurations but with similar impedance characteristics. Thus, the search space contains several local maxima of similar fitness, which indicates that the global GA is a suitable tool for this design problem.

In Section III-A, planar arrays without a groundplane were considered. It was shown that extremely broad-band designs could easily be obtained that performed well up to frequencies where grating lobe effects appear. A self-complementary array element was compared against a GA design, and it was found that the two elements have similar impedance characteristics although they differ in configuration.

A more challenging and, for practical reasons, more realistic problem is to consider groundplane backed arrays. The groundplane will constitute another bandwidth limiting factor at low frequencies in addition to the rapidly changing impedance at high frequencies due to the onset of grating lobes. As expected, if the substrate is made too thin (and thus the distance to the groundplane is made too small), the GA will have problems in finding an element well matched for all scan directions over a large frequency band. For a substrate thicker than about 0.1 λ_L, a bandwidth of at least one octave can be obtained for arrays scanned within 45° from broadside. The numerical simulations show that the bandwidth not necessarily increases with an increasing substrate thickness. By including the substrate thickness in the design procedure, a bandwidth of 2.23:1 was obtained with a substrate thickness of $d/\lambda_L \approx 0.11$.

The effect of electrical contact between neighboring elements has been investigated, and it was found to be only of minor benefit to array performance. This is perhaps not too surprising, since many of the unrestricted optimizations presented in this paper produced designs without direct conducting paths between the feed points of the neighboring elements. However, it is contrary to the conclusions drawn in [12]. Possibly, the explanation lies in the fact that [12] analyzed mainly arrays without groundplanes and for broadside scan only.

References

[1] H. Holter, T.-H. Chio, and D. H. Schaubert, "Elimination of impedance anomalies in single- and dual-polarized endfire tapered-slot phased arrays," *IEEE Trans. Antennas Propag.*, vol. 48, no. 1, pp. 122–124, Jan. 2000.

[2] D. McGrath, "Numerical analysis of TEM horn arrays," in *Sensor and Simulation Notes*. Albuquerque, NM: Air Force Research Lab., 1998.

[3] J. J. Lee, S. Livingstone, and R. Koenig, "A low-profile wide-band (5:1) dual-pol array," *IEEE Antennas Wireless Propag. Lett.*, vol. 2, pp. 46–49, 2003.

[4] H. Holter, "A new type of antenna element for wide-band wide-angle dual polarized phased array antennas," in *Proc. IEEE Int. Conf. Phased Array Systems Technology*, Boston, MA, Oct. 2003, pp. 393–398.

[5] R. C. Hansen, "Dipole array scan performance over a wide-band," *IEEE Trans. Antennas Propag.*, vol. 47, no. 5, pp. 956–957, May 1999.

[6] B. A. Munk, *Finite Antenna Arrays and FSS*. New York: Wiley, 2003, ch. 6.

[7] K. Kalbasi, R. Plumb, and R. Pope, "An analysis design tool for a broadband dual feed circles array antenna," in *Proc. IEEE AP-S Int. Symp. URSI Radio Science Meeting*, Chicago, IL, 1992, pp. 2085–2088.

[8] J. G. Teti Jr, W. D. Jemison, S. H. Kim, J. E. Laska Jr., and H. M. Halpern, "Wideband airborne early warning (AEW) radar," in *Proc. IEEE Nat. Radar Conf.*, Apr. 1993, pp. 239–244.

[9] B. Prepère and J. Hérault, "Conformal broadband phased array antenna," in *Proc. 2nd Eur. Workshop Conformal Antennas*, The Hague, The Netherlands, Apr. 2001.

[10] B. A. Munk *et al.*, "A low-profile broadband phased array antenna," in *Proc. Antennas Propagation Soc. Int. Symp.*, Columbus, OH, Jun. 2003, pp. 448–451.

[11] F. J. Villegas, T. Cwik, Y. Rahmat-Samii, and M. Manteghi, "A parallel electromagnetic genetic-algorithm optimization (EGO) application for patch antenna design," *IEEE Trans. Antennas Propag.*, vol. 52, pp. 2424–2435, 2004.

[12] P. Friedrich, L. Pringle, L. Fountain, P. Harms, G. Smith, J. Maloney, and M. Kesler, "A new class of broadband planar apertures," in *Antenna Application Symp.*, Allerton Park, IL, Nov. 2001, pp. 561–587.

[13] Y. Rahmat-Samii and E. Michielssen, *Electromagnetic Optimization by Genetic Algorithms*. New York: Wiley, 1999.

[14] H. Holter, "Analysis and design of broadband phased array antennas," Ph.D. dissertation, Royal Inst. of Technology, Stockholm, Sweden, 2000.

[15] Y. Mushiake, "The input impedance of a slit antenna," *Joint Conv. Rec. Tohoku Sections Inst. Elect. Eng. IEICE Jpn.*, pp. 25–26, Jun. 1948.

[16] ——, "Self-complementary antennas," *IEEE Antennas Propag. Mag.*, vol. 34, pp. 23–29, Dec. 1992.

[17] H. A. Wheeler, "Simple relations derived from a phased-array antenna made of an infinite current sheet," *IEEE Trans. Antennas Propag.*, vol. AP-13, no. 4, pp. 506–514, Jul. 1965.

[18] B. Thors and H. Steyskal, "Synthesis of broadband fragmented aperture array elements using genetic algorithms," Alfvén Lab., Royal Inst. of Technology, Stockholm, Sweden, Tech. Rep. TRITA-TET 2004:3, 2004.

Björn Thors received the M.Sc. degree in engineering physics from Uppsala University, Sweden, in 1996 and the Ph.D. degree in electromagnetic theory from the Royal Institute of Technology (KTH), Stockholm, Sweden, in 2003.

Since 2003, he has been a Research Associate with KTH. He spent the 2001 to 2002 academic year with the ElectroScience Laboratory, The Ohio State University, Columbus, as a Visiting Scholar, working with development of high-frequency methods for conformal antennas. From 2003 to 2005, he was a Research Associate at KTH. He is currently with Ericsson Research, Stockholm, Sweden, working with human exposure to radio frequency electromagnetic fields. His research interests include conformal antennas, scattering, high-frequency techniques, and broad-band array antennas.

Hans Steyskal (M'76–SM'91–F'96) received the Civ. Ing., Tekn. Lic., and Tekn. Dr. degrees in electrical engineering from the Royal Institute of Technology (KTH), Stockholm, Sweden in 1963, 1970, and 1973, respectively.

In 1962, he joined the Swedish National Defence Research Establishment (FOA), where he investigated microwave radiation and scattering problems. In 1980, he left his position as Chief of the Section for Field and Circuit Theory, and relocated to the United States. He is currently with the Air Force Research Laboratory (AFRL), Hanscom AFB, MA, where he was recently appointed Senior Scientist of Antennas. During 1996 to 2004, he held a part-time position as an Adjunct Professor in Antenna Technology at KTH. He has been a Visiting Scientist at the Polytechnic University of New York and The Federal Institute of Technology, Lausanne, Switzerland. His research interests include electromagnetics, phased array antennas, digital beamforming, and array signal processing.

Dr. Steyskal is an AFRL Fellow. He has served two terms as Associate Editor for the IEEE TRANSACTION ON ANTENNAS AND PROPAGATION.

Henrik Holter received the M.Sc.E.E. degree and the Ph.D. degree in electromagnetic theory from the Royal Institute of Technology, Stockholm, Sweden, in 1996 and 2000, respectively.

He served in the Swedish Navy from 1986 to 1996, where he attained the rank of "Kapten." In 1999, he spent six months at the Antenna Laboratory, University of Massachusetts, Amherst, participating in research on tapered slot antenna elements for phased arrays. He is currently with the Antenna Section at Saab Bofors Dynamics, Stockholm, working on broad-band array antennas and other types of antennas. He is author of about 30 journal and conference publications in the areas of broad-band array antennas and computational electromagnetics for array antennas.

Dr. Holter was named Best Graduate of the Year by the Royal Institute of Technology in 1996.